Monolithic MOFs for Carbon Capture

CCUS Innovation 2.0

Key Knowledge Deliverable 2.1, 3.2, 3.4 & 2.5.

Contents

1. Background

Work Package 2 of the CCUS project (WP2) is dedicated to engineering design and optimisation of a scalable CO_2 capture system that can be retrofitted to existing “high concentration” (i.e., ≥15%) point sources of flue gas such as coal-fired power plants, cement and steel factories. In this context, WP2 aims to develop a novel adsorption-based process system using two different generations of adsorption reactors (Gen.1 and Gen.2) which are tuned for operation of Immaterial’s proprietary monolithic metal-organic frameworks (*m*-MOFs). The system can recover CO_2 from feed streams and concentrate it with ≥96% purity, while at the same time maximising productivity of the process. As part of the above objectives, WP2 obtains and analyses important technical information regarding cycle configurations, and key performance indicators (KPIs) of the designed process for a given set of operating conditions. The engineering knowledge obtained from this work package will be crucial for the detailed design and building of a demonstrator unit that can be commissioned in collaboration with our industry partners in a separate phase of the project.

2. Adsorbent Selection and Choice of the Process Cycle

The first step in design of an adsorption-based carbon capture system is the choice of an appropriate process cycle based on properties of available adsorbents, and conditions of the flue gas. For this purpose, we considered adsorption behaviour of Immaterial’s top 3 adsorbent materials, namely IMM-16, IMM-16h, and IMM-28 whose synthesis and material properties are described in separate deliverable reports for WP1 and WP3. Equilibrium adsorption isotherms of these materials for CO_2 and N_2 (two major components of the flue gas) are shown in Figure 1. As evident from this figure, IMM-16 appears to have the desired characteristics of an ideal adsorbent for CO_2 capture in terms of total uptake, shape, Henry’s law constant, and selectivity over N_2.

The next step in the design of an adsorption separation system is associated with the choice of an appropriate process cycle that can realize maximum potential of the selected adsorbent. For this, we have designed a pressure-vacuum swing adsorption (PVSA) process using two generations of reactor beds that are optimized based on adsorption characteristics of Immaterial’s IMM-16 adsorbent.

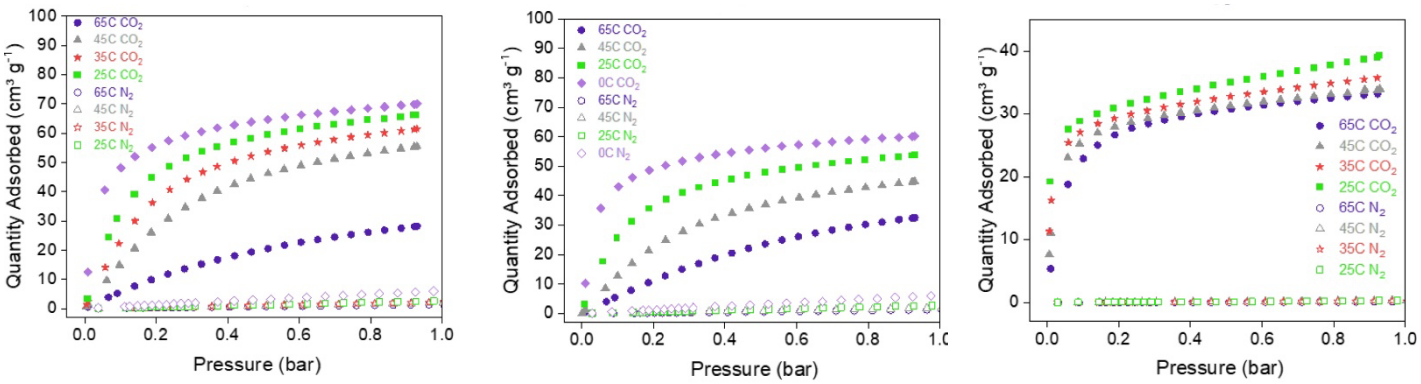

Figure 1. single-component adsorption isotherms of CO_2 and N_2 for IMM-16, IMM-16h and IMM-28 at different temperatures.

3. System Engineering Design of the PVSA Process

3.1. Model Construction

Modelling and optimization of the PVSA process constitute two major activities of WP2 which are preceded by a series of prerequisite tasks including collation of physical property data, numerical modelling of adsorption equilibrium data, bed engineering, and cycle scheduling.

3.1.1. Collation of Physical Property Data

Process modelling of swing adsorption systems require a large set of input data and parameters that are either obtained from experimental measurements or established through available theories. The most important set of data required for process modelling and optimization of PVSA systems include bed porosity, bed dimensions and geometry, pellet density, pellet heat capacity and thermal conductivity, equilibrium gas adsorption and isosteric heat of adsorption data for all components of the feed; mass transfer coefficients associated with intraparticle diffusion of adsorbate molecules, and fluid heat capacity and thermal conductivity. While details of the experimental data are reported in a separate document related to deliverable D3.1, here we only focus on analysis of the data as required for process modelling and optimization of the PVSA process.

3.1.2. Numerical Fitting of Equilibrium Adsorption Data

Equilibrium adsorption isotherms of two main components of dry feed (CO_2 and N_2) are measured experimentally up to 1 bar at different temperatures (Figure 1). Isotherms with temperatures relevant to operating conditions of the process were then fitted to an appropriate numerical adsorption model so that they can be used by our process modelling tool for interpolation of the data as required. We have fitted sub-atmospheric experimental adsorption isotherms of CO_2 and N_2 at 3 different temperatures using a dual-site Langmuir adsorption (DSL) model, results of which are presented in

Figure 2. The DSL model as described by eq. (1) is a powerful tool for correlating multicomponent gas adsorption data to single-component adsorption isotherms [1].

$$q_i^* = \sum_{j=1}^{2} \left[q_{j,i}^s \frac{b_{j,i} P}{1 + b_{j,i} P} \right] \qquad \text{eq. (1)}$$

In this equation, q_i^* denotes total gas uptake, $q_{j,i}$ is saturation capacity of site *j* with respect to species *i*, and $b_{j,i}$ describes affinity of each site. The DSL model has been shown to be a simple and yet adequate model for fitting type-I adsorption isotherms of simple gases such as CO_2, N_2, and O_2 [2-4] which has been widely adopted by the scientific community for modelling adsorption processes in the context of carbon capture.

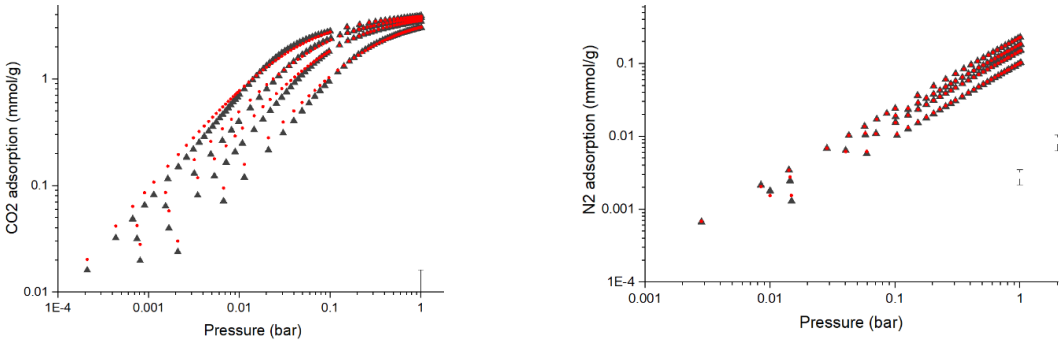

Figure 2. experimental (black) and DSL-fitted (red) adsorption isotherms of CO_2 and N_2 in IMM-16 at 3 different temperatures

From Figure 2, it is evident that the DSL model (red symbols) can provide an accurate fitting of the experimental data (black symbols) within the pressure range of interest.

3.1.3. Gen.1 Reactor Design

Sizing of the reactor is the main part of bed engineering. This is where maximum theoretical capacity and footprint of the process system is determined. The other important aspect of bed engineering is related to defining physical limitations of the bed in terms of the amount of feed flow that can be processed without fluidizing the bed. In our Gen.1 design, total volume of the reactor is $0.75\ m^3$ ($L = 1.5\ m, D = 0.8\ m$) with aspect ratio of $\frac{L}{D} = 1.875$. The bed is assumed to be packed with unisize spherical pellets of *m*-MOFs. Further details of the reactor bed are provided in Table 1.

Table 1. physical properties of Gen.1 adsorption reactor

Pellet diameter	Pellet density	Pellet porosity	Bed density	Bed porosity	Bed length	Bed diameter	Bed volume	Minimum fluidization velocity	Porosity at fluidization
3 $(\boldsymbol{mm})$	1240 $(\frac{kg}{m^3})$	0.23 $(-)$	744 $(\frac{kg}{m^3})$	0.4 $(-)$	1.5 (m)	0.8 (m)	0.75 (m^3)	0.52 $(\frac{m}{s})$	0.415 $(-)$

It should be noted that we have designed our system for feed streams containing 15% CO_2 and 85% N_2 on dry basis with total flowrate of 1642 kg/hr. There are normally small mole fractions of other gas components in the feed including water vapour, oxygen, SOx, NOx and various particulates depending on the feed source. Our assumption for using a binary feed mixture consisting of CO_2/N_2 is valid because with exception of oxygen, all other components will be removed from the feed using pre-treatment units located upstream of the carbon capture system. Pre-treatment units such as dehumidifiers or SOx and NOx scrubbers are standard unit operations that are commercially available, and their design is outside the scope of the current project. As for oxygen, adsorption behaviour of this component is known to be similar to that of nitrogen; hence its mole fraction in the feed is combined with that of N_2 in our modelling study.

The design provided in this section results in a system with an insignificant pressure drop (i.e., 1.8 kPa) across the bed for the given flowrate of the feed. This is a favourable figure because low pressure-drops would allow a non-energy intensive PVSA process to be constructed for the system of interest. The pressure-drop profiles of the bed versus superficial velocity, and flowrate of the feed are illustrated in Figure 3.

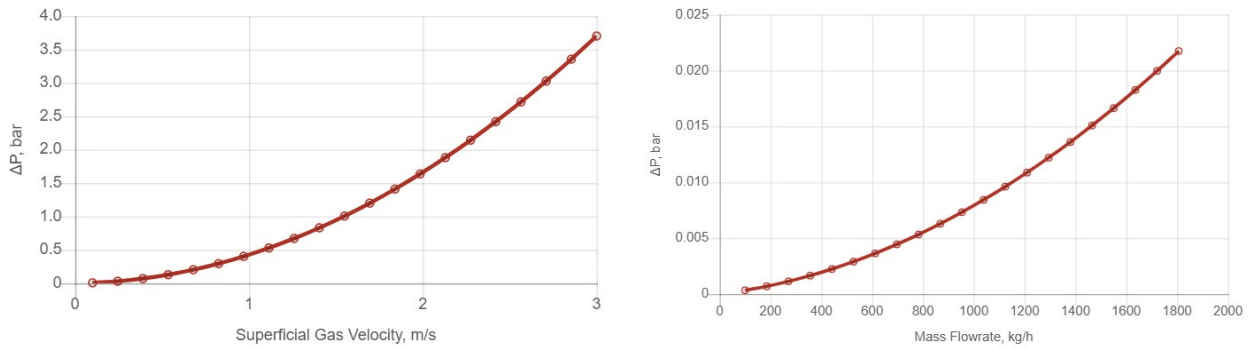

Figure 3. pressure-drop across the bed with respect to superficial gas velocity and flow rate of the feed

3.1.4. Cycle Design

We have considered various process configurations and compared them with those already reported in the literature [5-10]. Having reviewed different aspects of these processes, we ultimately designed a new PVSA cycle which was later optimized based on Immaterial's top-performing *m*-MOFs.

The proposed PVSA cycle consists of various consecutive steps from which only the typical steps are described below:

1) **Adsorption or feeding step:** At this step the reactor is exposed to feed during which CO_2 is selectively adsorbed by *m*-MOF, while N_2 leaves the bed as effluent from the product end of the reactor.
2) **Blowdown:** Pressure is reduced during Bd to intermediate pressures in order to remove N_2 from the bed, hence improving purity of CO_2 in the subsequent evacuation step.
3) **Evacuation:** This is when pressure of the bed is reduced even further using a vacuum pump to collect concentrated CO_2 as product.
4) **Re-pressurization:** the bed is repressurized after the evacuation up to the level required for the start of adsorption step in the next cycle.

To simulate performance of the PVSA cycle, a process model was developed where each of the cycle steps are explicitly implemented.

3.1.5. Cycle Scheduling

PVSA cycles often require multiple reactor beds to achieve the desired separation. At the same time, to maximize productivity of the carbon capture plant, it is preferred to construct a system with continuous flow, meaning at any given time at least one of the reactor beds should undergo a feeding step. To allow continuous feeding of the system, while matching relevant flow streams between interacting beds, a careful cycle schedule must be designed. The minimum number of columns required to implement the cycle in this way is called a "*train*". The cycle schedule designed for our PVSA process is very rapid and does not include any idle steps resulting in high gravimetric and volumetric productivities. It should be emphasized that the above train constitutes the most fundamental unit of our carbon capture system. For large-scale commercial plants, parallel trains must be simultaneously utilized to handle large flowrates of the feed. The design of a multi-train capture plant is outside the scope of the current demonstrator design.

3.2. Dynamic Behaviour and Optimization of the System with Gen.1 Reactor

To fully understand dynamic behaviour of the system, an extensive set of breakthrough measurements are required. These measurements will provide crucial information about breakthrough time and mass transfer limitations of adsorbent material which will be then used to adjust duration of different steps and estimate mass transfer coefficients of CO_2 and N_2. These measurements are carried out as part of WP3.

Process optimization is generally a challenging task for multi-steps PVSA cycles where a large set of decision variables contributes to overall performance of the system. Here, purity and recovery of CO_2 defined by eq. (2) and eq. (3), are considered as process objectives which must be simultaneously maximized.

$$\text{purity} = \frac{\text{total mol } CO_2 \text{ in extract product}}{\text{total mol } CO_2 \text{ and } N_2 \text{ in extract product}} \times 100 \qquad \text{eq. (2)}$$

$$\text{recovery} = \frac{\text{total mol } CO_2 \text{in extract product}}{\text{total mol } CO_2 \text{fed into cycle}} \times 100 \qquad \text{eq. (3)}$$

Eleven decision variables are considered in our process optimization resulting in a highly multi-dimensional optimization space. These variables include duration of all steps; various stream flowrates; as well as blowdown and evacuation pressures. Figure 4 illustrates the outcomes of a number of different optimization trials with respect to purity and recovery of the PVSA process. The chosen cycle schedule also adds an additional constraint on duration of each step; hence only configurations that satisfy these constraints can be accepted. The best purity and recovery of CO_2 (purity = 96%, recovery = 86%) for the chosen cycle schedule is shown by a blue diamond symbol in Figure 4. Evidently, the CO_2 product captured by our carbon capture unit meets the 96% minimum purity specification of the transfer and storage (T&S) infrastructure as defined in the CCUS Innovation 2.0 call by the Department of Business, Energy & Industrial Strategy (BEIS).

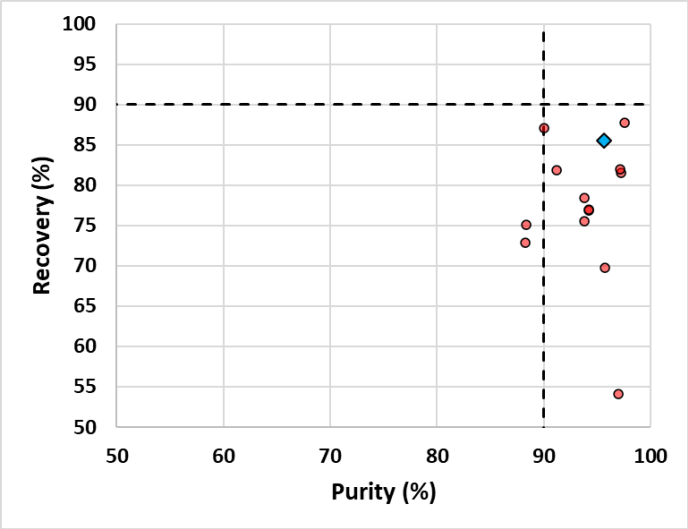

Figure 4. purity and recovery of the PVSA cycle for different optimization trials. Best configuration fulfilling the cycle schedule is shown by a blue diamond symbol.

Another important KPI in the design and optimization of separation processes is productivity of the process as described by the following equation:

$$\text{productivity} = \frac{\text{total mol } CO_2 \text{ in extract product}}{(\text{total volume of adsorbent}) \times (\text{cycle time})} \qquad \text{eq. (4)}$$

Currently, for the given process configuration with purity = 96% and recovery = 86%, productivity of the Gen.1 demonstrator train is 7.32 $\frac{tonne\ of\ CO2}{day}$. On annual basis, a single CO_2 capture unit designed in this work will be able to capture 2,670 tonne of CO_2 which will require 1.68 tonne of IMM-16.

3.3. Dynamic Behaviour and Optimization of the System with Gen.2 Reactor

The Gen.2 adsorption reactor is designed based on Immaterial's proprietary structured adsorbent form factor where heat and mass transfer properties of adsorbents are significantly improved compared to pelletized *m*-MOFs. Gen.2 reactor design is used to enhance process productivity through the implementation of rapid cycles. At the same time, the new design aims to reduce overall energy consumption of the process by minimizing pressure drop across the beds. Table 2 summarizes physical properties of the Gen.2 reactor.

Table 2. physical properties of Gen.2 adsorption reactor

Bed density	Bed porosity	Bed length	Bed diameter	Bed volume	Pressure drop
100 - 170 $(\frac{\boldsymbol{kg}}{\boldsymbol{m^3}})$	0.7 – 0.8 $(-)$	1.5 (m)	0.8 (m)	0.75 (m^3)	2 - 5 $(mbar)$

To better understand adsorption kinetic of CO_2 and N_2 gas mixtures in Gen.1 and Gen.2 reactors of *m*-MOFs, we have conducted a detailed analysis of relevant gas diffusivities which include estimation of Knudsen and molecular diffusivities along with macropore, effective macropore, and effective pellet diffusivities [5]. Here, the goal was to estimate mass transfer coefficients (MTC) of CO_2 and N_2 as obtained from the linear driving force (LDF) model [5] which must be otherwise extracted from fitting of experimental breakthrough curves, the data that are being measured as part of WP3. The theoretical MTCs calculated in this work will serve as a good starting point for our dynamic process modelling, also providing a reliable basis to compare with the experiments. The results from these analyses suggest that mass transfer rates estimated using LDF model are >400 times larger in Gen.2 structured adsorbents compared to those associated with Gen.1 MOF pellets.

To intensify our PVSA cycle, a suitably sized Gen.2 reactor was incorporated into the process in which the new reactor contained 127 kg of IMM-16 in different forms of structured adsorbent. By capitalizing on rapid mass transfer kinetic of CO_2 and N_2 in structured forms of IMM-16, we were able to increase feed flow rate by a factor of 4, while attempting to simultaneously reduce total cycle time. Significantly faster mass transfer through structured *m*-MOFs improves bed utilization through sharpening of adsorbed-phase CO_2 front in the reactor. In our Gen.2 reactor, we were able to increase feed flowrate of the system by a factor of 4 without increasing bed dimensions which in turn suggests a shorter residence time is achievable. A shorter residence time allows us to reduce duration of adsorption step without any CO_2 breaking through from the bed. This observation is shown in Figure 5 where adsorbed-phase profiles of Gen.1 and Gen.2 reactors are compared. It should be noted that in this figure the Gen.1 reactor has been on feed for 100 seconds (left figure), however, for the system with Gen.2. design, the feeding time is reduced to 25 seconds!

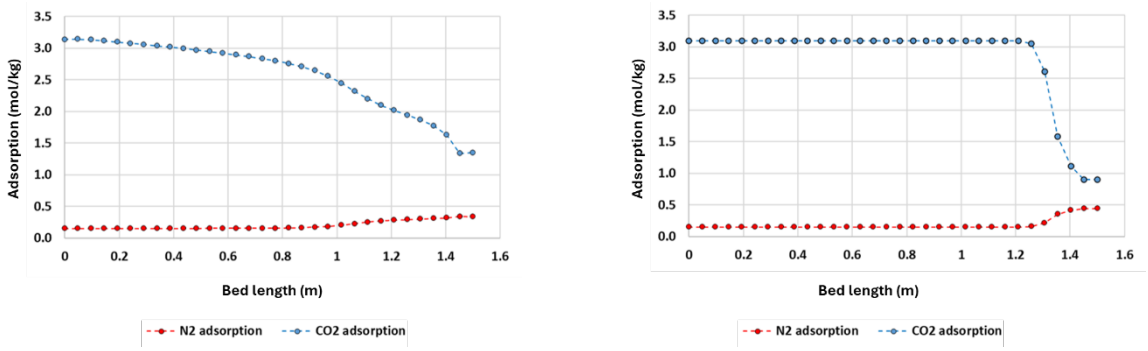

Figure 5. Comparison of adsorbed-phase front in Gen.1 (left) and Gen.2 (right) adsorption reactors. Blue and red curves represent CO_2 and N_2 concentrations respectively.

To achieve maximum productivity, we have intensified performance of our PVSA cycle through incorporation and optimization of the Gen.2 reactor design. The intensified cycle shows a dramatic increase in gravimetric productivity (by a factor of 18) which is the result of simultaneous improvement on multiple fronts including increased feed flowrate, reduced cycle time, enhanced mass transfer, and higher bed utilization. The intensified PVSA unit is now capable of capturing **29** $\frac{\textbf{kte CO2}}{\textbf{te MOF.year}}$ at **98%** purity and **90%** recovery meeting the scales required for building a commercial CO_2 capture plant. Figure **6** compares the results of process optimization for Gen.1 and Gen.2 PVSA systems.

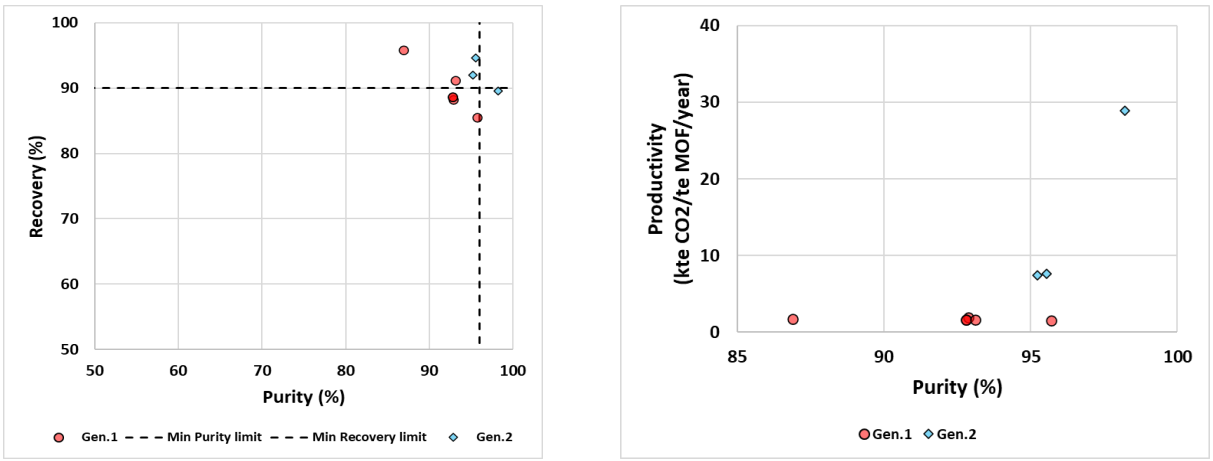

Figure 6. Comparison of system's performance between Gen.1 (red symbols) and Gen.2 (blue symbols) designs.

4. Sensitivity Analysis of the PVSA Process

This section is dedicated to sensitivity analysis of the PVSA system. Here, we report on the outcome of a series of sensitivity analyses carried out to better understand the complex interplay between different process variables and their collective or individual impacts on overall system's performance.

4.1. Understanding the Impact of Blow down and Evacuation Steps

N_2 and CO_2 products are produced during blow down (Bd) and evacuation (Evac) steps of the process. Bd and Evac pressures along with duration of each step dictate purity of N_2 and CO_2 products respectively. We performed sensitivity analysis to understand the impact of these cycle variables on purity and recovery of the system, the results of which are shown in Figure 7.

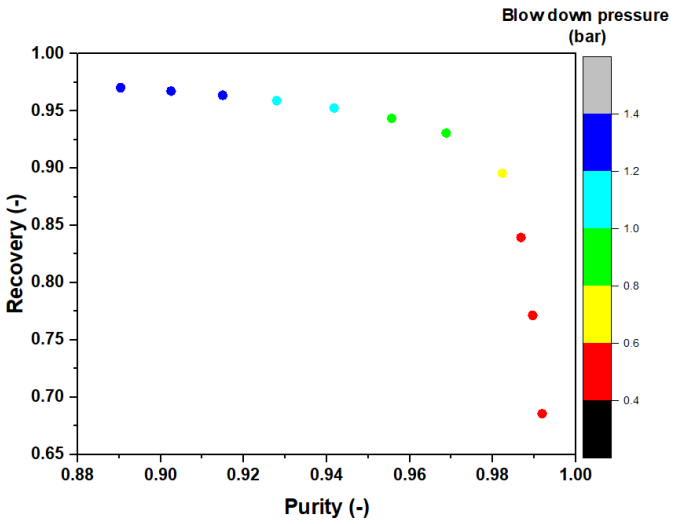

Figure 7. Variation of CO_2 purity and recovery with respect to blow down pressure

As demonstrated by this figure, CO_2 purity is enhanced at lower P_{bd} due to N_2 being almost completely removed from the product stream before the evacuation step. Lower P_{bd}, however, results in lower CO_2 recovery considering CO_2 starts to desorb at these pressures and hence leaving the bed along with N_2. This analysis also suggests the optimum value of P_{bd} to be around 0.76 bar.

Another set of sensitivity analyses focused on the impact of blow down and evacuation step times on purity and recovery of CO_2, with their corresponding results illustrated in Figure 8.

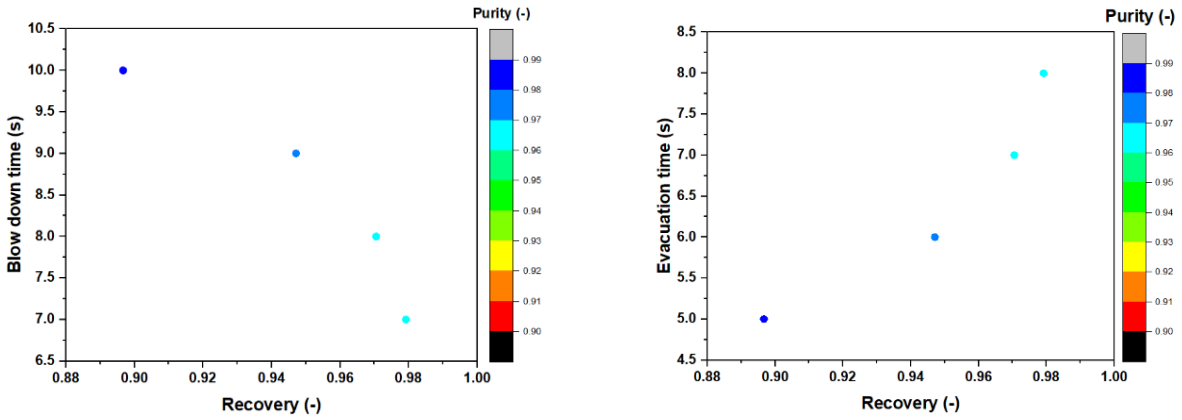

Figure 8. Variation of CO_2 purity and recovery with respect to duration of blow down and evacuation steps

According to the right panel of Figure 8, CO_2 recovery is enhanced when evacuation step is almost 8 seconds (as opposed to original t_{evac} = 5). Longer t_{evac} helps to achieve a slightly lower pressure by the end of evacuation step resulting in the removal (desorption) of more CO_2 from the bed. Considering the total duration of blow down and evacuation steps cannot be larger than 15 seconds, this consequently means a shorter step time for blow down (7 seconds as opposed to 10 sec used originally) which will impact CO_2 purity negatively (left panel). The overall picture is consistent with our understanding that purity and recovery of the system are two competing KPIs that cannot be improved simultaneously.

We have also analysed the impact of blow down and evacuation step times on CO_2 mass hold-up in the reactor by looking at the variation of this variable with respect to different step-times for blow down and evacuation steps as shown in Figure 9.

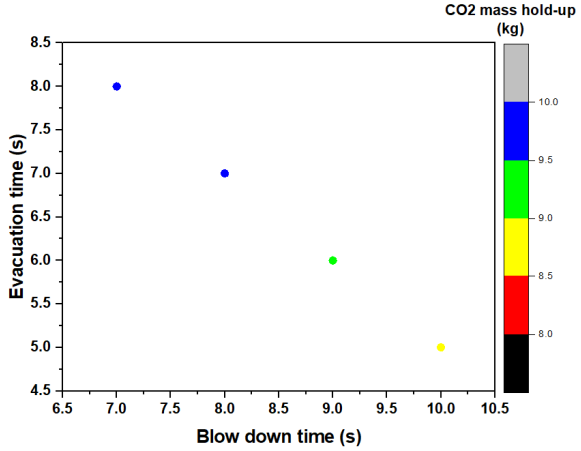

Figure 9. Variation of CO_2 mass hold-up with respect to duration of blow down and evacuation steps

Here, CO_2 mass holdup is higher when evacuation step time is around 8 seconds which is correlated to the higher recovery value achieved at this step-time according to Figure 8.

4.2. Impacts of Bed Porosity on System's KPIs

We have extended our sensitivity analysis to investigate the impact of porosity and the amount of available active materials on system's KPIs. Higher porosity normally means a larger volumetric fraction of the bed is empty (less adsorbent material available) and lower bed porosity will have the opposite effect. Varying bed porosity also affects pressure drop across the bed. We have examined performance of the system for 3 different bed porosities at a fixed cycle configuration. Results of this analysis are provided in Table 3 with a visual presentation of productivity figures shown in Figure 10.

Table 3. System's KPIs for Gen.1 reactor design at different bed porosities

Bed Porosity (-)	Mass of MOF (kg)	Pressure-drop (bar)	Purity (-)	Recovery (-)	Volumetric Productivity ($kg/m^3/h$)	Gravimetric Productivity ($kg/kg_{MOF}/h$)
0.2	748	0.213	0.87	0.85	135	0.135
0.4	561	0.018	0.87	0.96	152	0.203
0.6	374	0.003	0.92	0.91	145	0.290

From the results presented in Table 3, it is evident that 300% increase in bed porosity only reduces the amount of adsorbent in the reactor by 50%. This, however, does not guarantee a monotonic increase of volumetric productivity. In contrast, since higher porosity essentially corresponds to a decrease in the amount of active material, gravimetric productivity monotonically increases within the porosity range investigated here as shown in Figure 10.

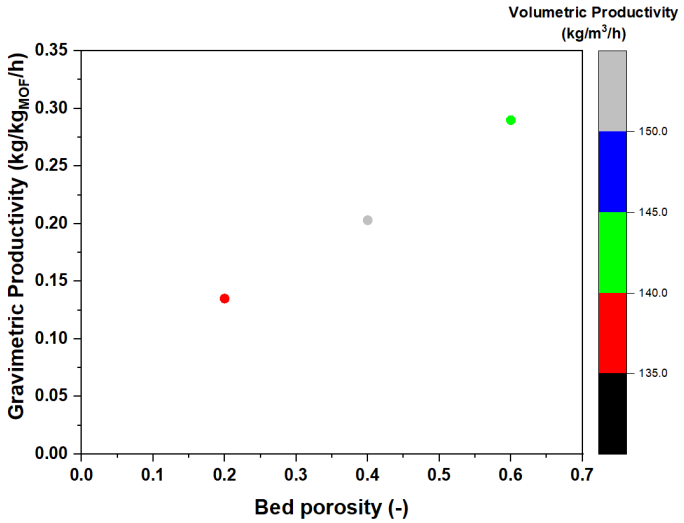

Figure 10. Impact of Gen.1 reactor porosity on productivity of the system

For the Gen.2 reactor design, the picture is distinctly different. In these reactors, bed porosity and mass of adsorbent can be varied by using different forms of structured materials (form factor). We have analysed system's performance for four different form factors for which the results are presented in the following.

Table 4. System's KPIs for Gen.2 reactor design at different reactor porosities

Form Factor	Bed Porosity (-)	Mass of MOF (kg)	Volumetric Productivity ($kg/m^3/h$)	Gravimetric Productivity ($kg/kg_{MOF}/h$)
Form 1	0.74	127	567.6	3.3
Form 2	0.74	98	491.0	3.8
Form 3	0.77	115	497.3	3.2
Form 4	0.78	109	529.3	3.7

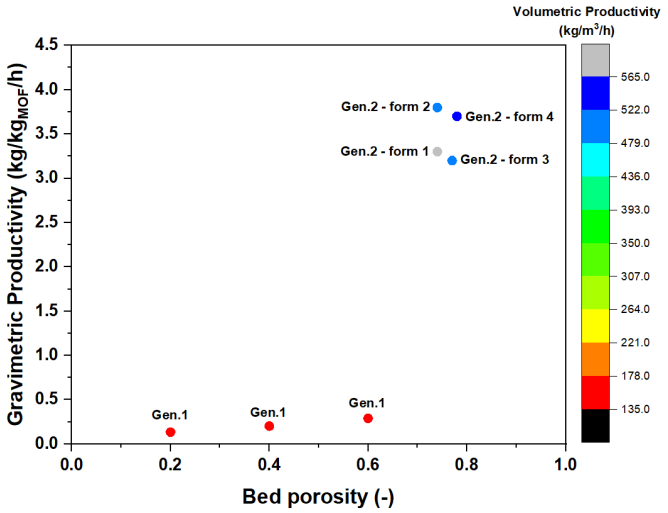

Figure 11. Impact of bed porosity on system's productivity for Gen.1 and Gen.2 (various form factors) designs

As shown in Figure 11, we can change the amount of adsorbent in the bed simply through changing the reactor porosity and form factor of our structured adsorbents.

5. Concluding Remarks

In this report, we have presented a summary of our journey for the design of two subsequent generations of our PVSA carbon capture system. We have initially carried out an experimental materials screening campaign through which 3 top performing *m*-MOFs were identified. We then selected IMM-16 as the most suitable candidate for our PVSA process. This MOF was produced in different form factors and used in two different reactor designs (Gen.1 and 2). Our modelling studies confirmed that the Gen.2 system outperforms its Gen.1 counterpart by a factor of 18 in terms of gravimetric productivity. The intensified process was shown to reach a capture capacity of **29** $\frac{\textbf{kte CO2}}{\textbf{te MOF.year}}$ at **98%** purity and **90%** recovery levels which is suitable for commercial-scale applications. We complemented our report by a series of sensitivity analyses where the impact of various process variables and their complex interplay on overall system's performance was investigated. In a separate work package, Immaterial has carried out a large set of experiments to validate the modelling results reported here. We will also be seeking to demonstrate our carbon capture system design in a pilot scale through collaboration with our industry partners.

Glossary

Ads	Adsorption
Bd	Blow Down
DSL	Dual Site Langmuir
Evac	Evacuation
KPI	Key Performance Indicator
LDF	Linear Driving Force
m-MOF	Monolithic Metal Organic Frameworks
MTC	Mass Transfer Coefficient
PVSA	Pressure Vacuum Swing Adsorption
T&S	Transport and Storage
TPD	Tonne Per Day
WP	Work Package

References

1. Mathias, P.M., et al., *Correlation of Multicomponent Gas Adsorption by the Dual-Site Langmuir Model. Application to Nitrogen/Oxygen Adsorption on 5A-Zeolite.* Industrial & Engineering Chemistry Research, 1996. **35**(7): p. 2477-2483.

2. Ritter, J.A., S.J. Bhadra, and A.D. Ebner, *On the Use of the Dual-Process Langmuir Model for Correlating Unary Equilibria and Predicting Mixed-Gas Adsorption Equilibria.* Langmuir, 2011. **27**(8): p. 4700-4712.

3. Ritter, J.A., et al., *On the use of the dual process Langmuir model for binary gas mixture components that exhibit single process or linear isotherms.* Adsorption, 2019. **25**(8): p. 1511-1523.

4. Farmahini, A.H., et al., *From Crystal to Adsorption Column: Challenges in Multiscale Computational Screening of Materials for Adsorption Separation Processes.* Industrial & Engineering Chemistry Research, 2018. **57**(45): p. 15491-15511.

5. Farmahini, A.H., et al., *Performance-Based Screening of Porous Materials for Carbon Capture.* Chemical Reviews, 2021. **121**(17): p. 10666-10741.

6. Peh, S.B., S. Farooq, and D. Zhao, *A metal-organic framework (MOF)-based temperature swing adsorption cycle for postcombustion CO2 capture from wet flue gas.* Chemical Engineering Science, 2022. **250**: p. 117399.

7. Nguyen, T.T.T., et al., *Separation of CO2 and N2 on a hydrophobic metal organic framework CALF-20.* Chemical Engineering Journal, 2022. **442**: p. 136263.

8. Nguyen, T., G.K.H. Shimizu, and A. Rajendrana, *Post-Combustion CO2 capture by vacuum swing adsorption using a hydrophobic metal-organic framework (MOF), CALF-20: Multi-objective optimization and experimental validation.* ChemRxiv, 2022.

9. Bo Peh, S., S. Farooq, and D. Zhao, *Techno-Economic Analysis of MOF-Based Adsorption Cycles for Postcombustion CO2 Capture from Wet Flue Gas.* Chemical Engineering Science, 2022: p. 118390.

10. Subraveti, S.G., et al., *How much can novel solid sorbents reduce the cost of post-combustion CO2 capture? A techno-economic investigation on the cost limits of pressure–vacuum swing adsorption.* Applied Energy, 2022. **306**: p. 117955.

This publication is available from: www.gov.uk/desnz

If you need a version of this document in a more accessible format, please email alt.formats@energysecurity.gov.uk. Please tell us what format you need. It will help us if you say what assistive technology you use.